Figure S1

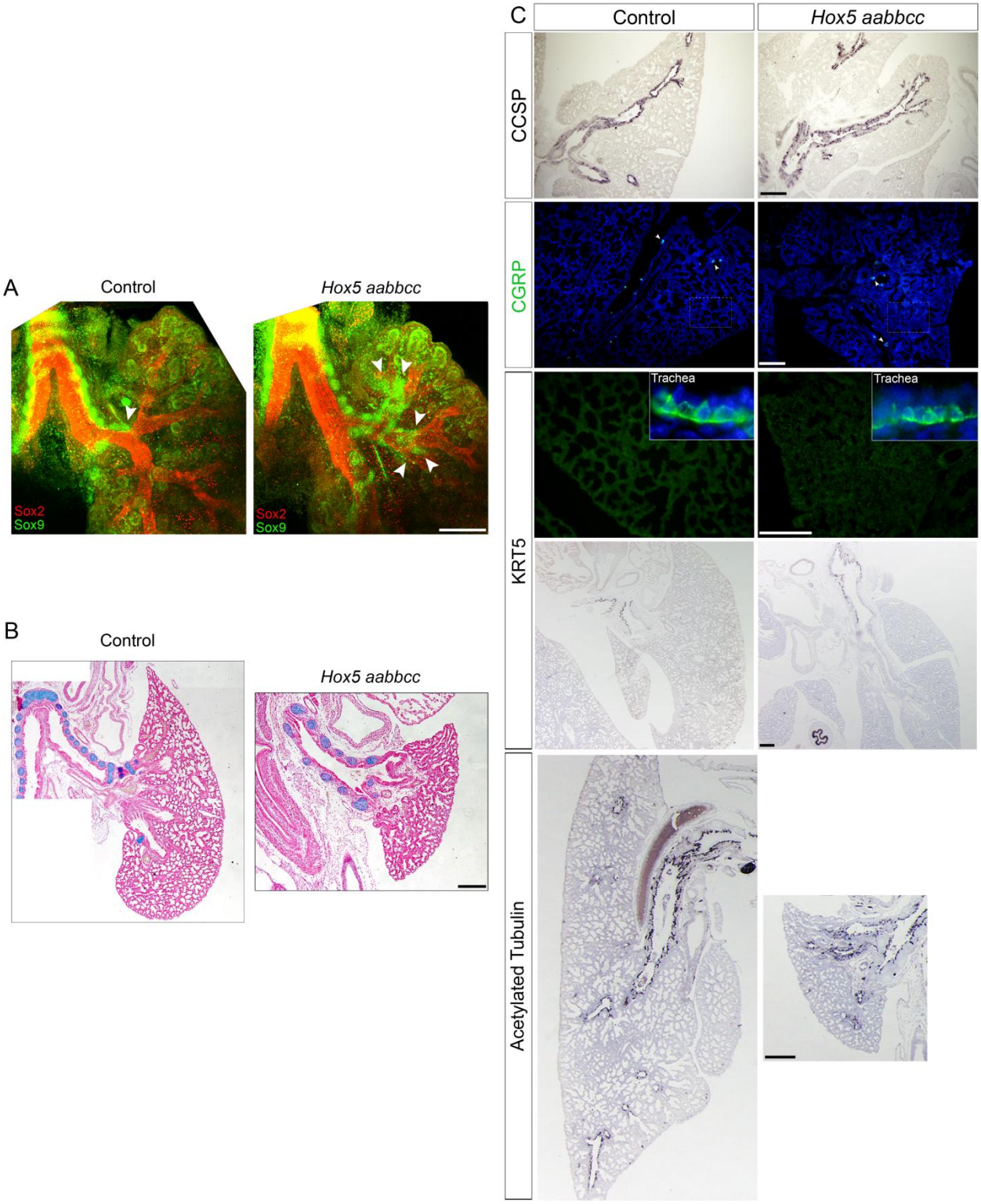
A
Control
Hox5 aabbcc
Sox2
Sox9
Sox2
Sox9
B
Control
Hox5 aabbcc
C
Control
Hox5 aabbcc
CCSP
CGRP
KRT5
Trachea
Trachea
Acetylated Tubulin

Figure S1. There are no defects in the distribution of proximal cell types in *Hox5* triple mutants despite the mesenchymal expansion of Sox9. Related to Figure 1.

(A) Sox2/Sox9 WM IHC performed in control and *Hox5* triple mutant E14.5 lungs. Mesenchymal Sox9 expression in *Hox5* mutants extends into more distal regions of the lung compared to control (white arrowheads). Scale bar represents 50uM for both panels.

(B) Alcian blue staining of control and *Hox5* triple mutant lungs at E18.5 shows there is no observable ectopic cartilage present in the lung of *Hox5* triple mutants. Scale bar represents 200uM in both panels

(C) Analysis of markers for proximal lung cell types in *Hox5* triple mutant lungs at E18.5. The overall distribution of club cells (CCSP+), PNEC cells (CGRP+), ciliated cells (Acetylated Tubulin+) and basal cells (KRT5+) are unaffected in *Hox5* triple mutants. In addition, there is no ectopic expression of any of the above proximal markers in the distal airway of *Hox5* triple mutants. Scale bars represent 200uM in all panels.

Figure S2

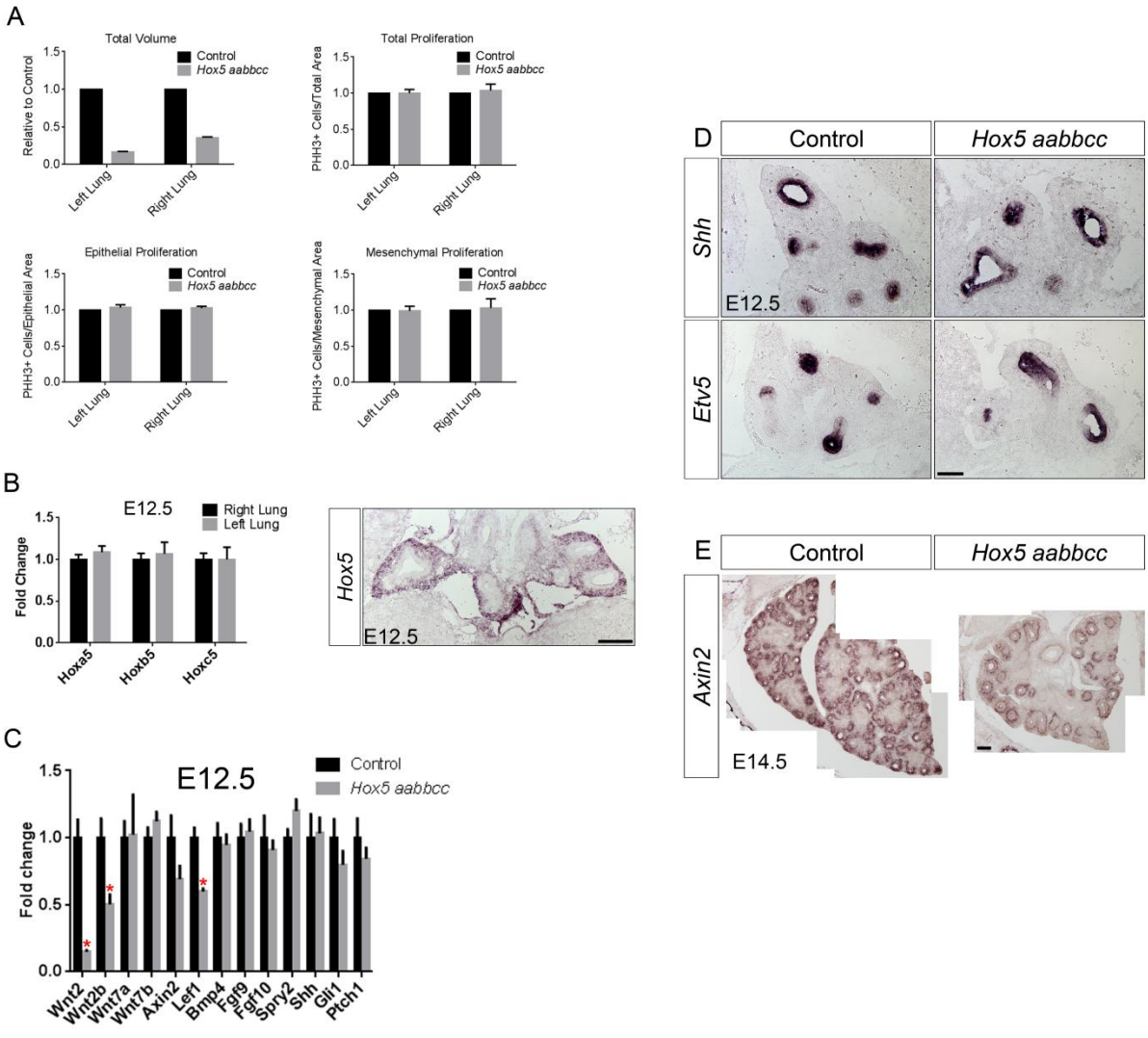
A
Total Volume
Relative to Control
Control
Hox5 aabbcc
Left Lung
Right Lung
Total Proliferation
PHH3+ Cells/Total Area
Epithelial Proliferation
PHH3+ Cells/Epithelial Area
Mesenchymal Proliferation
PHH3+ Cells/Mesenchymal Area
B
E12.5
Right Lung
Left Lung
Fold Change
Hoxa5
Hoxb5
Hoxc5
Hox5
C
Fold change
Wnt2
Wnt2b
Wnt7a
Wnt7b
Axin2
Lef1
Bmp4
Fgf9
Fgf10
Spry2
Shh
Gli1
Ptch1
D
Shh
Etv5
E
Axin2
E14.5

Figure S2. Analysis of proliferation, expression of *Hox5* and members of key pathways in *Hox5* triple mutant lungs. Related to Figure 2.

(A) Entire lungs of control and *Hox5* triple mutant lungs at E14.5 were sectioned and every section was stained for DAPI. Quantification of total DAPI area using ImageJ software reveals that the total volume of the left and right lobes of *Hox5* triple mutants are reduced ≈85% and ≈65%, respectively, compared to controls. Proliferation was analyzed by comparing total number of PHH3+ cells/Total DAPI area in the lung mesenchyme and epithelium of controls and *Hox5* triple mutants at E14.5. Our data show no differences in the proliferation rates in either the lung mesenchyme and/or epithelium in *Hox5* triple mutants at E14.5.

(B) qPCR analyses of *Hoxa5*, *Hoxb5* and *Hoxc5* in control lungs at E12.5 show no difference in the expression levels of any of the *Hox5* genes in the left and right lobes. ISH analyses using probes to all three *Hox5* genes show uniform expression in both the right and left lobes at E12.5. Scale bar represents 200uM.

(C) qPCR analyses show a reduction in the expression levels of the two mesenchymal Wnt ligands, *Wnt2* and *Wnt2b*, and downstream targets of Wnt signaling including *Axin2* and *Lef1* in *Hox5* triple mutants at E12.5. The expression levels of the two epithelial Wnt ligands *Wnt7a* and *Wnt7b*, *Bmp4* and all components of the Fgf and Shh signaling pathways examined were unchanged at E12.5.

(D) ISH analyses of *Etv5*, a downstream read-out of Fgf signaling and *Shh* show no perturbations in levels or patterns in *Hox5* triple mutants compared to controls at E12.5. Scale bar represents 100uM for all panels.

(E) Stitched 10X images of *Axin2* ISH analyses at E14.5 in control and *Hox5* triple mutants. *Axin2* expression is specifically absent in the distal epithelium throughout the entire lobe although mesenchymal expression appears unchanged in *Hox5* triple mutants. Scale bar represents 100uM in both panels.

Figure S3

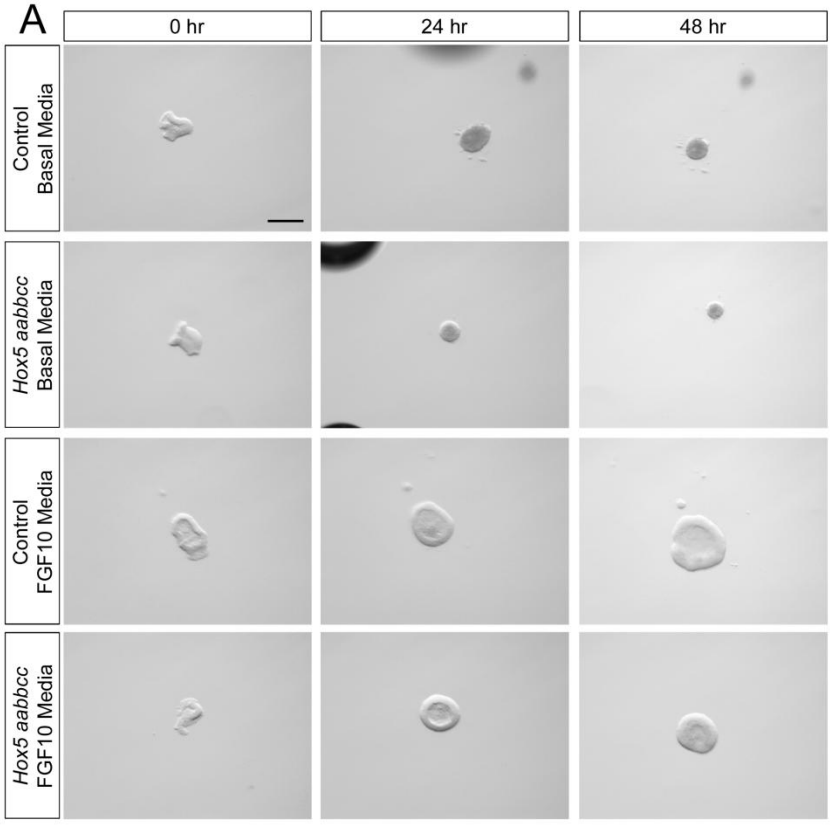

Scale bar represents 100μm

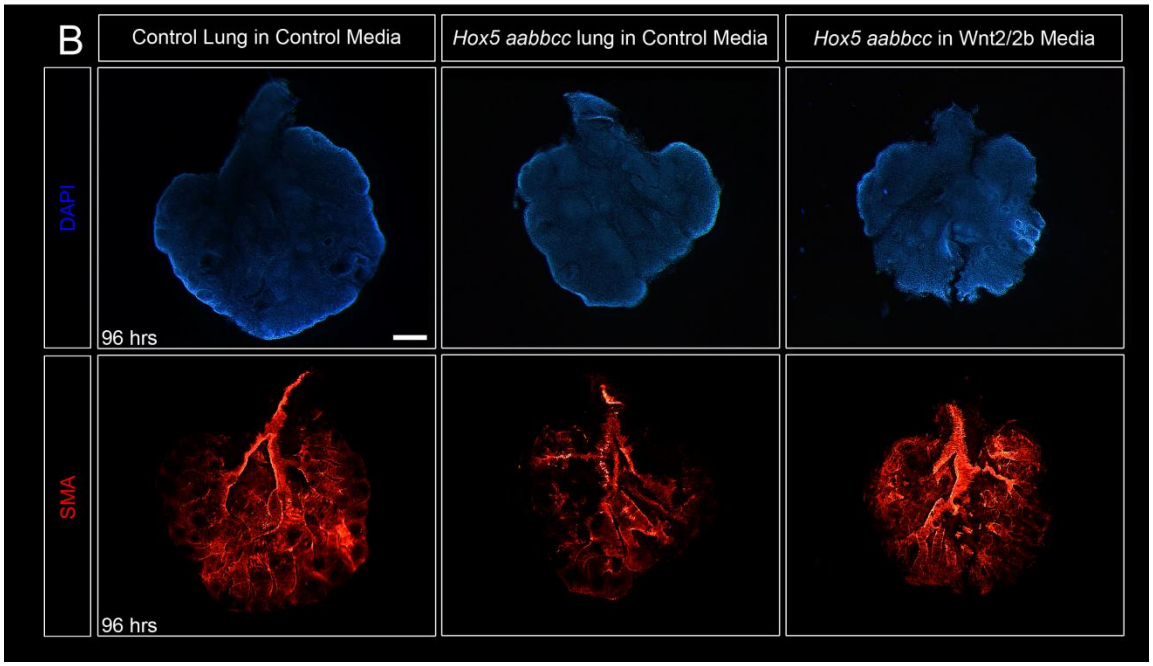

Figure S3: Dissected lung epithelium of *Hox5* triple mutants respond normally to Fgf10 and treatment of *Hox5* lung explants with Wnt2/2b ligand restores proper smooth muscle development. Related to Figure 4.

(A) Dissected lung epithelial buds from control and *Hox5* triple mutant animals at E12.5 were cultured in Matrigel with and without Fgf10 for 48 hrs. Both E12.5 control and mutant epithelia respond equivalently in the presence or absence of Fgf10.

(B) WM SMA immunostaining of *Hox5* triple mutant explants cultured in control media shows a marked decrease, and in some areas absence, of SMA expression, similar to what is observed *in vivo*. Treatment of *Hox5* triple mutant explants with *Wnt2/2b* ligand restores proper smooth muscle development. Scale bar represents 200uM for all panels.

Figure S4

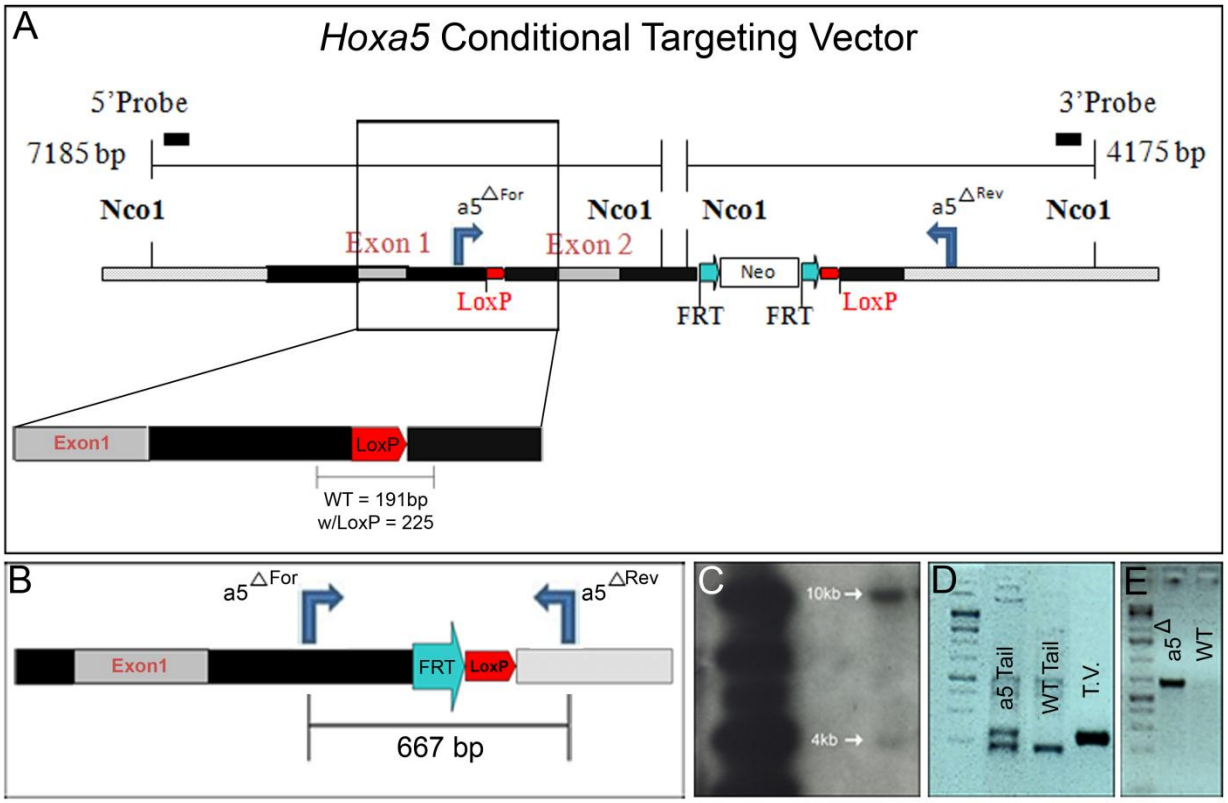
A
Hoxa5 Conditional Targeting Vector
5'Probe
7185 bp
3'Probe
4175 bp
Nco1
a5ΔFor
Nco1
Nco1
a5ΔRev
Nco1
Exon 1
Exon 2
Neo
LoxP
FRT
FRT
LoxP
Exon1
LoxP
WT = 191bp
w/LoxP = 225
B
a5ΔFor
a5ΔRev
Exon1
FRT
LoxP
667 bp
C
10kb
4kb
D
a5 Tail
WT Tail
T.V.
E
a5Δ
WT

Figure S4. Generation of *Hoxa5* mutant mice. Related to the Mice and Histology section in the Experimental Procedures.

(A) Diagram of *Hoxa5* targeting vector. LoxP sites flanking exon 2 were inserted into the *Hoxa5* allele to facilitate removal upon Cre-mediated recombination. Arrows indicate position of primers used to determine if Cre-mediated recombination occurred. Boxed region shows a magnified view of the targeting vector where the LoxP primers were designed.

(B) Diagram of the *Hoxa5* conditional locus following Cre-mediated recombination. Blue arrows indicate primer sites used to PCR screen for recombination events.

(C) Southern blot following NcoI digestion of electroporated ES cell DNA showing the presence of both WT (10kb) and conditional *Hoxa5* (4kb) bands indicating successful targeting.

(D) PCR of tail samples from generated mice using primers indicated in (A, boxed region) showing proper insertion of LoxP sites.

(E) PCR of tail samples from generated mice using primers indicated in (B) showing successful Cre-mediated recombination.

Table S1

Gene	Forward Primer	Reverse Primer
HoxA5	CAGGGTCTGGTAGCGAGTGT	CTCAGCCCCAGATCTACCC
HoxB5	CTGGTAGCGAGTATAGGCGG	AGGGGCAGACTCCACAGATA
HoxC5	TTCTCGAGTTCCAGGGTCTG	ATTTACCCGTGGATGACCAA
FGF10	GCAACAACTCCGATTTCCAC	GATTGAGAAGAACGGCAAGG
Spry2	AGAGGATTCAAGGGAGAGGG	CATCAGGTCTTGGCAGTGTG
Gli1	GGATGAGAGAGCAGTTGGGA	ATTGGATTGAACATGGCGTC
Ptch1	CTCCTCATATTTGGGGCCTT	AATTCTCGACTCACTCGTCCA
Wnt2	CCAACGAAAAATGACCTCGT	GGGAAGTCAAGTTGCACACA
Wnt2b	CTGCTGCTGCTACTCCTGACT	GGGGATGTTGTCACAGATCA
Wnt7a	TACACAATAACGAGGCGGGT	TGTGGTCCAGCACGTCTTAG
Wnt7b	ACGTGTTTCTCTGCTTTGGC	CCAGGCCAGGAATCTTGTT
Lef1	AAATGGGTCCCTTTCTCCAC	CTCGTCGCTGTAGGTGATGA
Axin2	TGCATCTCTCTCTGGAGCTG	ACTGACCGACGATTCCATGT
Bmp4	TGGACTGTTATTATGCCTTGTTT	CTCCTAGCAGGACTTGGCAT
FGF9	ACGAGAAGGGGGAGCTGTAT	AGAGGTTGGAAGAGTAGGTGTTG

Table S1: List of primers used for qPCR analyses.

Supplemental Experimental Procedures

Generation of Hoxa5 mutant mice:

BAC clone RP23-20F21 spanning the entire *HoxA* complex was identified by screening the RPCI-23 C57Bl/6 library (Osoegawa et al., 2000). 10 kb of genomic sequences including coding sequence for *Hoxa5*, 3.3 kb upstream of exon 1 and 3.9 kb downstream of exon 2 was sub-cloned into the pBluescript SK (+) vector. *LoxP* sites flanking exon 2 of the *Hoxa5* allele were inserted 567 bp downstream of exon 1. An frt-flanked NEO-bGHpA cassette (Stratagene) followed by a second *LoxP* in the same orientation as the first *LoxP* site was inserted 374 bp downstream of the 3' UTR. Figure S4A, B shows a schematic of the *Hoxa5* targeting vector.

The *Hoxa5* targeting vector was electroporated into R1 ES cells (Nagy et al., 1993) and G418 selection was performed. Surviving clones were analyzed by Southern blot analysis to identify homologous recombinants using a 5′ flanking probe and a 3′ flanking probe (Figure S4A). A ~550 bp 5' probe was generated using primers 5' AAC TGG TTG AGA TGA GAA AGC C 3' and 5' TGG GGA GAG TTT AAG CTC TAA A 3'. The ~500 bp 3' probe was generated using primers 5' GCT ATT CGG CTA TGA CTG GGC ACA 3' and 5' GCC CTA GGA ATG TAT TTG GTT GGA 3' and randomly labeled with ^{32}P-dCTP. Southern blot analyses following NcoI digestion of ES cell DNA allowed identification of successful targeted clones (Figure S4C). Two positive clones were identified, confirmed for euploidy and injected into blastocysts. Twelve high-percentage, agouti chimeric founders were generated; a single founder successfully transmitted the allele. PCR primers 5' TAA AAG GGG CTT GGG GGG AAT T 3' and 5' TTT TCT CAG TTC CCA AGT GGC 3' flanking the *LoxP* sites of the *Hoxa5* conditional allele were used to analyze tail DNA and confirmed proper insertion and germ-line transmission of both *LoxP* sites (Figure S4D). *Hoxa5*$^{Flox/+}$ females were first crossed to FlpO (Wu et al., 2009) mice to allow deletion of Neo^{r} cassette; this was confirmed by PCR surrounding deleted cassette (data not shown). Resulting female mice were subsequently mated to Cre-ERT2/+ males (Feil et al., 1997; Lois et al., 2002) and given tamoxifen IP injections at E8.5 and E9.5. Tail DNA was collected from pups and Cre-mediated recombination across *LoxP* sites was confirmed by PCR analysis using the following primers: 5' ATT TAT GGG AAG GGC TAC AC 3' and 5' ATG TCA ACT CCC CAA AAC CA 3' (Figure S4E). Resulting *Hoxa5*$^{\Delta/+}$ mice were then crossed into our previously described existing *Hoxb5* and *Hoxc5*

mutant colonies to generate *Hox5* triple mutant mice, and animals from this line as well as previously reported *Hox5* alleles were used in this study (McIntyre et al., 2007).

In situ hybridization and Immunohistochemistry:

Section ISH was performed as previously described (Di Giacomo et al., 2006; Mendelsohn et al., 1999). All *in situ* probes used in this report were previously described (Echelard et al., 1993; Herriges et al., 2012; Jones et al., 1991; Miller et al., 2012; Xu et al., 2013; Yallowitz et al., 2011). Tissue sections were stained with the following antibodies and dilutions: anti-Sox9 (Millipore; 1:500), anti-Sox2 (Santa Cruz; 1:100); anti-E-cad (R&D Systems; 1:100), anti-Aqp5 (Abcam; 1:400), anti-SP-B (Santa Cruz; 1:250), anti-Nkx2.1 (Abcam; 1:800), anti-SMA (Sigma-Aldrich, 1:400), anti-CCSP (Seven Hills, 1:1000), anti-acetylated tubulin (Sigma-Aldrich, 1:1000), anti-CGRP (Sigma-Aldrich, 1:400), anti-KRT5 (Abcam, 1:500).

Lung bud cultures

Isolation of epithelial buds from the surrounding mesenchyme of E12.5 lungs and culture was previously described (del Moral et al., 2006; Del Moral and Warburton, 2010). Briefly, E12.5 mouse lung was isolated and treated with undiluted dispase (Corning, CB-40235) for 30 min on ice followed by a15 min incubation in FBS (Corning 35-015-CV) on ice. The distal mesenchyme was separated from the distal epithelium using fine tungsten needles and the epithelial buds were transferred into a Matrigel™ (BD Biosciences) droplet. Droplet was overlaid with DMEM/Ham's F-12 supplemented with 50 U/mL penicillin-streptomycin and 5% (vol/vol) FBS (Corning) with and without 500 ng/ml of FGF10 (R&D, 345-FG-025). Epithelial buds were maintained at 37 °C in a 5% CO2 incubator for 48hrs.

References:

del Moral, P.M., De Langhe, S.P., Sala, F.G., Veltmaat, J.M., Tefft, D., Wang, K., Warburton, D., and Bellusci, S. (2006). Differential role of FGF9 on epithelium and mesenchyme in mouse embryonic lung. Dev Biol *293*, 77-89.

Del Moral, P.M., and Warburton, D. (2010). Explant culture of mouse embryonic whole lung, isolated epithelium, or mesenchyme under chemically defined conditions as a system to evaluate the molecular mechanism of branching morphogenesis and cellular differentiation. Methods Mol Biol *633*, 71-79.

Di Giacomo, G., Koss, M., Capellini, T.D., Brendolan, A., Popperl, H., and Selleri, L. (2006). Spatio-temporal expression of Pbx3 during mouse organogenesis. Gene Expr Patterns *6*, 747-757.

Echelard, Y., Epstein, D.J., St-Jacques, B., Shen, L., Mohler, J., McMahon, J.A., and McMahon, A.P. (1993). Sonic hedgehog, a member of a family of putative signaling molecules, is implicated in the regulation of CNS polarity. Cell *75*, 1417-1430.

Feil, R., Wagner, J., Metzger, D., and Chambon, P. (1997). Regulation of Cre recombinase activity by mutated estrogen receptor ligand-binding domains. Biochem Biophys Res Commun *237*, 752-757.

Herriges, J.C., Yi, L., Hines, E.A., Harvey, J.F., Xu, G., Gray, P.A., Ma, Q., and Sun, X. (2012). Genome-scale study of transcription factor expression in the branching mouse lung. Dev Dyn *241*, 1432-1453.

Jones, C.M., Lyons, K.M., and Hogan, B.L. (1991). Involvement of Bone Morphogenetic Protein-4 (BMP-4) and Vgr-1 in morphogenesis and neurogenesis in the mouse. Development *111*, 531-542.

Lois, C., Hong, E.J., Pease, S., Brown, E.J., and Baltimore, D. (2002). Germline transmission and tissue-specific expression of transgenes delivered by lentiviral vectors. Science *295*, 868-872.

McIntyre, D.C., Rakshit, S., Yallowitz, A.R., Loken, L., Jeannotte, L., Capecchi, M.R., and Wellik, D.M. (2007). Hox patterning of the vertebrate rib cage. Development *134*, 2981-2989.

Mendelsohn, C., Batourina, E., Fung, S., Gilbert, T., and Dodd, J. (1999). Stromal cells mediate retinoid-dependent functions essential for renal development. Development *126*, 1139-1148.

Miller, M.F., Cohen, E.D., Baggs, J.E., Lu, M.M., Hogenesch, J.B., and Morrisey, E.E. (2012). Wnt ligands signal in a cooperative manner to promote foregut organogenesis. Proc Natl Acad Sci U S A *109*, 15348-15353.

Nagy, A., Rossant, J., Nagy, R., Abramow-Newerly, W., and Roder, J.C. (1993). Derivation of completely cell culture-derived mice from early-passage embryonic stem cells. Proc Natl Acad Sci U S A *90*, 8424-8428.

Osoegawa, K., Tateno, M., Woon, P.Y., Frengen, E., Mammoser, A.G., Catanese, J.J., Hayashizaki, Y., and de Jong, P.J. (2000). Bacterial artificial chromosome libraries for mouse sequencing and functional analysis. Genome Res *10*, 116-128.

Wu, Y., Wang, C., Sun, H., LeRoith, D., and Yakar, S. (2009). High-efficient FLPo deleter mice in C57BL/6J background. PLoS One *4*, e8054.

Xu, B., Hrycaj, S.M., McIntyre, D.C., Baker, N.C., Takeuchi, J.K., Jeannotte, L., Gaber, Z.B., Novitch, B.G., and Wellik, D.M. (2013). Hox5 interacts with Plzf to restrict Shh expression in the developing forelimb. Proc Natl Acad Sci U S A *110*, 19438-19443.

Yallowitz, A.R., Hrycaj, S.M., Short, K.M., Smyth, I.M., and Wellik, D.M. (2011). Hox10 genes function in kidney development in the differentiation and integration of the cortical stroma. PLoS One *6*, e23410.